Journal of King Saud University – Science 34 (2022) 102284

HOSTED BY

Contents lists available at ScienceDirect

Journal of King Saud University – Science

journal homepage: www.sciencedirect.com

Original article

# Green synthesis and pharmacological applications of silver nanoparticles using ethanolic extract of *Salacia chinensis* L.

Madhuranthakam Reddi Nagesh [a], Nirubama Kumar [b], Javed Masood Khan [c], Mohammad Z. Ahmed [d], R. Kavitha [e], Sung-Jin Kim [f], Natesan Vijayakumar [a,*]

[a] Department of Biochemistry and Biotechnology, Faculty of Science, Annamalai University, Annamalainagar 608002, Tamil Nadu, India
[b] Department of Biochemistry, Kongunadu Arts and Science College, Coimbatore 641029, Tamil Nadu, India
[c] Department of Food Science and Nutrition, Faculty of Food and Agricultural Sciences, King Saud University, 2460, Riyadh 11451, Saudi Arabia
[d] Department of Pharmacognosy, College of Pharmacy, King Saud University, Riyadh, Saudi Arabia
[e] Department of Biotechnology, Periyar University PG Extension Centre, Dharmapuri 636701, Tamil Nadu, India
[f] Department of Pharmacology and Toxicology, Metabolic Diseases Research Laboratory, School of Dentistry, Kyung Hee University, Seoul 02447, Republic of Korea

ARTICLE INFO

*Article history:*
Received 19 March 2022
Revised 25 June 2022
Accepted 15 August 2022
Available online 20 August 2022

*Keywords:*
Silver nanoparticles
*Salacia chinensis L*
Antimicrobial
Antiproliferation
HEK293 cell lines

ABSTRACT

*Objectives:* In recent years, biological precursor-based synthesis, particularly plant-based green synthesis, has piqued attention in the area of nanotechnology. The goal of this work is to look into the antibacterial, antifungal, antioxidant, and antiproliferation activity of silver nanoparticles (AgNPs) made from ethanolic extract of *Salacia chinensis* L. were investigated.
*Methods:* This study can be broadly separated into three parts: the first extraction from *Salacia chinensis* L. roots, The second characterization of NPs by UV-Vis, DLS, FTIR and SEM, and the third analysis of its antimicrobial; antioxidant and antiproliferative properties. UV–Vis absorption indicated the synthesis of AgNPs, and the spectrum was seen at 401 and 447 nm. The existence of functional groups in the produced AgNPs was verified by FT-IR spectral peaks at 3423.83 $cm^{-1}$. In three planes, XRD was calculated to investigate the crystallinity and consistent spherical size (peaks at 2θ values of at 28.78, 32.18, 38.04, 54.63, and 77.08°) of the particles.
*Results:* The results of antibacterial, antifungal and antiproliferative effect of synthesized AgNPs with *Salacia chinensis* L. ethanolic root extract have admirable antimicrobial (19.5 mm), antioxidant ($IC_{50}$ values 117.3, 59.61 g $mL^{-1}$) and antiproliferative activity against HEK293 cell lines protect up to 90.3 % respectively.
*Conclusions:* As a consequence, biosynthesized *Salacia chinensis* L. AgNPs shown outstanding effects and have the potential to be used as antibacterial, antioxidant, and antiproliferative agents.


## 1. Introduction

Nanoscience is the study of the distinct characteristics of materials with dimensions ranging from 1 to 100 nm. Nanomaterials seem to be applying such findings to the creation or modification of new things (Rodríguez-Félix et al., 2021; Tapia-Hernández et al., 2019a). Also, Nanotechnology is considered a multidisciplinary science that aids in solving current problems and is defined as the control of matter at the atomic and molecular levels (Tapia-Hernández et al., 2019b; Tapia-Hernández et al., 2018). Nanoparticles are an important advance in medicine and healthcare, and it has been used to address some of the most frequent actions, such as antibacterial, antifungal, and antioxidant properties (Narayanan et al., 2021). Silver nanoparticles (AgNPs) are a developed nanomaterial widely used in antimicrobial and personal care products. Although several research on the synthesis and characterization of AgNPs have been published (Lee et al., 2013; Sukweenadhi et al., 2021). Synthesizing NPs using traditional methods is costly, hazardous, and detrimental to the environment. To overcome these difficulties, researchers discovered the specific green methodologies to make nanoparticles. (Gour and Jain, 2019; Balan et al., 2021; Samuggam et al., 2021).

Plants and its extracts have acquired appeal in green synthesis because of their rapid development, cost-effective, single-step

* Corresponding author.
*E-mail address:* nv12507@annamalaiuniversity.ac.in (N. Vijayakumar).
Peer review under responsibility of King Saud University.

Production and hosting by Elsevier

https://doi.org/10.1016/j.jksus.2022.102284

technique, non-pathogenicity, and ecologically beneficial characteristics (Egbuna et al., 2021). Roots, flowers, stems, leaves, shoots, barks, seeds, and their derivatives have been effectively utilized for nanoparticle biosynthesis (Khan et al., 2020). The plant components are made dependent on the quantity of functional phytoconstituents as phenolic compunds, flavonoids and other compounds. (Tapia-Hernández et al., 2018; Del-Toro-Sánchez et al., 2021). Agri-food wastes are also an important source of phytochemicals and their use in green synthesis reduces environmental pollution and gives them added value. (Rodríguez-Félix et al., 2022). *Salacia chinensis* L. (Saptarangi) is a highly valued climbing shrub of the Celastraceae family found widespread in South-East Asia, In India's Ayurvedic system of traditional medicine, it is known as Dimal, Modhupal, Ingli, Cherukuranti Saptarangi, and Saptachakra (Sudhakar et al., 2015; Keerawelle et al., 2019; Kartini et al., 2020). Triterpenes, amino acids, glycosides, coumarin, alkaloids, saponins, flavonoids, and tannins are among the phytoconstituents discovered in various portions of this plant (Chinnappan et al., 2018). Mangiferin, salacinol, and kotalanol were found in the roots as anticancer and anti-diabetic phytoconstituents (Gacem et al., 2019). *Salacia chinensis* L. (Sc) plant extracts were used to synthesise NPs, which were shown antifungal, antibacterial, antidiabetic, antioxidant, immunomodulating, anti-inflammatories, anti-HIV, and immunomodulatory characteristics (Cassir et al., 2014). With the aforementioned considerations in mind, the current work investigated AgNPs production employing an ecofriendly technique for efficient growth suppression of drug-resistant bacteria at small doses. Therefore, in this work, we have attempted to the biosynthesis of AgNPs from ethanolic root extracts of *Salacia chinensis* L. (*Sc*-AgNPs). As a result, the purpose of this work was to evaluate the activity and processes behind the effect of varied doses of *Sc*-AgNPs against microbial pathogens. Finally, antioxidant potential has been estimated using DPPH, ABTS assay and antiproliferation activity against HEK293 tumour cell lines.

## 2. Materials and methods

### 2.1. Collection of plant root and identification

The fresh root of *Salacia chinensis* L. was collected in June from the lower montane evergreen forest (latitude $11^0 10'$-$11^O 30'$ N○, and longitude of $78^0 37'$ –$78^0 51'$ E○) in the Kollimalai, Namakkal district, Tamil Nadu, India. Professor P. Jayaraman, Plant Anatomy Research Institute, West Tambram, Tamil Nadu, India, verified the root of *Salacia chinensis* L. (authentication no. PARC/2020/4259). The root of *Salacia chinensis* L. was collected in a sterile bag and transferred to the laboratory. The root sample was washed with tap water followed by distilled water. Secondly, shadow dried the cleaned root sample at room temperature (25 ± 2 $^0$C, Rh 50–60 %) for up to 25 days.

### 2.2. Root extract of Salacia chinensis L

The dried root sample as a whole was processed into a fine powder. Then the powdered material (10 g) was solvent-extracted with 200 mL of ethanol (Merck Chemicals) for rotary evaporator at 80$^0$C, 100 rpm for 4 hr. The extracts were filtered using Whatman filter paper before being utilised to make *Sc*-AgNPs and kept at 4 °C.

### 2.3. Biosynthesis of S.chinensis -AgNPs

*Sc*-AgNPs were synthesized by adding 2 mL of ethanolic extract of *Salacia chinensis* L. to 25 mL of 1 mmol mL$^{-1}$ silver nitrate (Qualigens) solution. They agitated the reaction mixture at 500 rpm for 36 hr at room temperature. The formation of *Sc*-AgNPs was detected visually and verified by UV visible spectrophotometer (Shimadzu Corporation). The nanoparticles mixture was purified by repeated centrifuged (Eppendorf) at 6000 rpm for 20 min, then decanted by residual sediment and dried at 60 $^0$C in an oven (Benchtop Instruments) for overnight. The thin coating of *Sc*-AgNPs that remained on the surface of the watch glass was used for characterization.

### 2.4. Characterization of Sc-AgNPs

The following approaches were used to characterize the synthesized silver nanoparticles. Maximal absorption of silver nanoparticles was scanned at resolutions of 1 nm between the wavelengths of 200 nm to 800 nm by a Double beam UV–visible spectrophotometer. DLS analysis (Microtrac Inc, USA) was performed to determine the average size of *Sc*-AgNPs. The functional group and biomolecules of synthesized *Sc*-AgNPs were detected by FT-IR in the 4000 cm$^{-1}$ to 500 cm$^{-1}$ range during its synthesis. The morphology, like particle size (average) and shape of AgNPs was analyzed by scanning electron microscopy (SEM) (Zeiss) with EDAX. The Purity and size of the *Sc*-AgNPs were analyzed by powder X-ray diffraction calculated by Debye–Scherrer formula and the width of the Bragg's reflection (Reda et al., 2019).

### 2.5. Antimicrobial activity

#### 2.5.1. Antibacterial activity

Agar well diffusion method was evaluated the maximal antibacterial effect of biosynthesized *Sc*-AgNPs from the root of *Salacia chinensis* L. Each petri plate containing 20 mL of nutrient agar medium (Himedia) was seeded with a 24 hr culture of pathogeneic bacterial strains (*Staphylococcus aureus*-902, *Streptococcus pyogenes* –1928, *Proteus vulgaris*-426 and *E.coli*-443) were obtained from MTCC (Microbial type culture collection), Chandigarh, India. Then 6 mm wells were whacked with wood borer, and different concentration of sample PR (500 µL, 250 µL, 100 µL, and 50 µL) was loaded into the wells against all media plates through a micropipette (Eppendorf). As a positive control, the antibiotic gentamicin (Himedia) was employed, while DMSO (Merck Chemicals) was used as a negative control. The plates were incubated at 37 °C for 24 h. Antibacterial activity was determined by measuring the width of the inhibition zone generated around the wells. Using the Graph Pad Prism 6.0 application, the diameter and radius were measured in millimetres and analysed. (Kebede et al., 2021).

#### 2.5.2. Antifungal activity

The fungal cultures *(*Aspergillus niger and Candida albicans*)* were maintained on potato dextrose agar medium (Himedia) (Kebede et al., 2021). The freshly prepared 20 mL PDA were seeded with 48 hr culture of (0.5 mL of *Aspergillus niger* and *Candida albicans*). Then, 6 mm wells were whacked with the wood borer and different concentrations of sample PR (500 µL, 250 µL, 100 µL, and 50 µL) into the wells against all media plates through a micropipette (Eppendorf). The antibiotic Amphotericin B (Himedia) was used as a positive control, and DMSO (Merck Chemicals) used as a negative control. The plates were incubated for 48–72 hr at 30 °C. The radius of the inhibitory zone was measured to determine antifungal activity. The diameter and radius were measured in mm and evaluated using the Graph Pad Prism 6.0.

### 2.6. Antioxidant activity

#### 2.6.1. DPPH assay

The DPPH radical scavenging assay was used to evaluate the antioxidant activity of the synthesized *Sc*-AgNPs from ethanolic

extracts of *Salacia chinensis* L. Accordingly, 300 µL of synthesized *Sc*-AgNPs at various concentrations (500, 400, 300, 200, 100, 80, 60, 40, 20 and 10 µg $mL^{-1}$) and standard ascorbic acid (Himedia). 100 µL of DPPH (Himedia) were added to the mixture (0.1 mM 2.6 mL of 2,2-DPPH) and incubated in dark for 30 min at RT with shaking using shaker incubator (Bench top Instruments). After 30 min, UV–Visible spectrophotometer was used to measure the colour absorbance at 517 nm and DPPH free radical scavenging percentage was calculated by (Al-Otibi et al., 2021).

$$\text{DPPH radical scavenging activity } (\%) = \frac{(\text{Absorbance of control} - \text{Absorbance of } Sc - \text{AgNPs})}{\text{Absorbance of control}} \times 100$$

*2.6.2. TS assay*

The ABTS scavenging activity of the synthesized *Sc*-AgNPs from ethanolic extracts of *Salacia chinensis* L was studied with standard protocol. Accordingly, 300 µL of synthesized *Sc*-AgNPs at various concentrations (500, 400, 300, 200, 100, 80, 60, 40, 20, and 10 µg $mL^{-1}$) and standard ascorbic acid were mixed with 1 mL of ABTS (Himedia) working solution and incubated for 30 min at room temperature. After 30 min, UV–Vis spectrophotometer was used to measure the absorbance at 734 nm. The ABTS free radical scavenging % activity was calculated using the methodology below (Jain and Mehata, 2017).

$$\text{ABTS radical scavenging activity } (\%) = \frac{(\text{Absorbance of control} - \text{Absorbance of } Sc - \text{AgNPs})}{\text{Absorbance of control}} \times 100$$

*2.6.3. Tiproliferation activity*

HEK293 cell lines (NCCS, Pune, India) were maintained in DMEM media (Himedia) enriched with 11 % FBS (Himedia), Amphotericin B (Himedia) (51 µg $mL^{-1}$), Penicillin (Himedia) (100 µg $mL^{-1}$) and Streptomycin (100 µg $mL^{-1}$). Cells (HEK293) were strained with fluorescent dye (acridine orange) and treated for 24 to 48 hr with various concentrations of biosynthesized *Sc*-AgNPs from ethanolic root extracts of *Salacia chinensis* L. (50, 100, 200, 300, 400, and 500 µg $mL^{-1}$) along with rutin (positive) and cisplatin (negative), respectively. Following that, the plates (in triplicates) were incubated in humidified $CO_2$ incubators at 37 °C for 2 hr. After incubation add Dimethyl sulfoxide (100 µg $mL^{-1}$) was added and % of cell viability was calculated and recording absorbance at 570 nm. The percentage of cell viability was determined using the standard formula (Gonfa et al., 2021).

$$\text{HEK293 viability } (\%) = \frac{(\text{Absorbance of acridine orange treated HEK293} - \text{Absorbance of DMSO})}{\text{Absorbance control HEK293} - \text{Absorbance Dimethyl sulfoxide}} \times 100$$

## 3. Results and discussion

### 3.1. Characterization of Sc-AgNPs

*3.1.1. UV–Visible absorption*

In this work, green synthesis of AgNPs was carried out under shaking conditions for 48 hr. As predicted, the color of the sample changed from pale yellow to brown during the reaction of Ag ions for subsequent formation of *Sc*-AgNPs, The time scale of *Sc*-AgNPs synthesis varied with $AgNO_3$ concentration (Fig. 1A), and experimental results indicate that the maximum concentration was used. *Sc*-AgNPs were produced after 24 hr at more silver nitrate concentrations, whereas lower silver nitrate concentrations required a longer time to detect a colour change. UV–Visible spectrophotometry represents absorption sharp peak at 447 nm, which as predicted the formation of *Sc*-AgNPs and has a close agreement with previous work (Behravan et al., 2019; Vijayakumar et al., 2022). As a result, in the current study, 48 hr was determined to be the optimum time scale for nanoparticle production. As intended, increasing the amount of extract resulted in a high number of flavonoids, terpenoids, and phenols, which exposed more $Ag^+$ ions resulted in increased absorption. However, these results agree well with existing studies on the increase in absorption (higher *Sc*-AgNPs) due to the reaction rate increase substantially supporting the synthesis of additional *Sc*-AgNPs, which may be related to their predicted aggregation maximum at 400 and 500 nm (Behravan et al., 2019; Vijayakumar et al., 2022).

*3.1.2. Dynamic light scattering pattern*

The polydispersity index (PDI) and hydrodynamic particle size distribution of biosynthesized *Sc*-AgNPs were evaluated using the dynamic light scattering (DLS) method. The organic shell also was taken into consideration by DLS when calculating the total size of the compounds in colloids or their overall hydrodynamic size. To decrease background scattering, the ethanolic silver nanoparticle sample was diluted suitably. The average particle size of biosynthesized *Sc*-AgNPs is generally non-uniform 172.6 nm, according to the size distribution graph, with a comparatively low polydispersity index of 0.313. (Fig. 1B). The hydrodynamic size of *Sc*-AgNPs encompasses the hydration coating on their exterior, which is superior to the size examined by SEM. The phytocompouds in the root extract may also have a role in the hydrodynamic size. These results agree well with existing studies on 150 nm hydrodynamic particle size and around 0.3 of PDI values, and different particle sizes are mostly determined by various phytocompounds found in solvent extracts (Nguyen et al., 2020).

*3.1.3. FTIR spectra*

Because of the capping, reduction, and stability of the synthesized *Sc*-AgNPs nanoparticles, the FTIR spectra confirmation of *Sc*-AgNPs exhibited large and small shifts of the bands. The primary major absorption bands were found at 3423.83 $cm^{-1}$ to 3401.23 $cm^{-1}$ of lowest wavelength (Fig. 2A), because of the participation of NH and OH group stretching of aromatic phenolic phytocompounds that are observed in the synthesized *Sc*-AgNPs. The CH group stretching of the aliphatic or, methylene leads to the strong absorption band at 2923.64 $cm^{-1}$ to a lower wavelength of 2853.38 $cm^{-1}$, which seems to be a typical band of saponins and triterpenoid. The high band indicated the existence of the CO stretching of tertiary alcohols or aromatic phenol at 1640.28 $cm^{-1}$; the lower band at 1383.99 $cm^{-1}$ indicated the presence of the OH stretching of the aromatic group. The CO and CS stretch and the participation of aliphatic groups or aliphatic chloro compounds were shown by the strong band at 1271.82 $cm^{-1}$. The signal at 1074.93 $cm^{-1}$ might be related to the aliphatic group's CH stretching, whereas the lower band shift of 617.08 $cm^{-1}$ indicated the aromatic group. The phenolic groups of triterpenoids, polyphe-

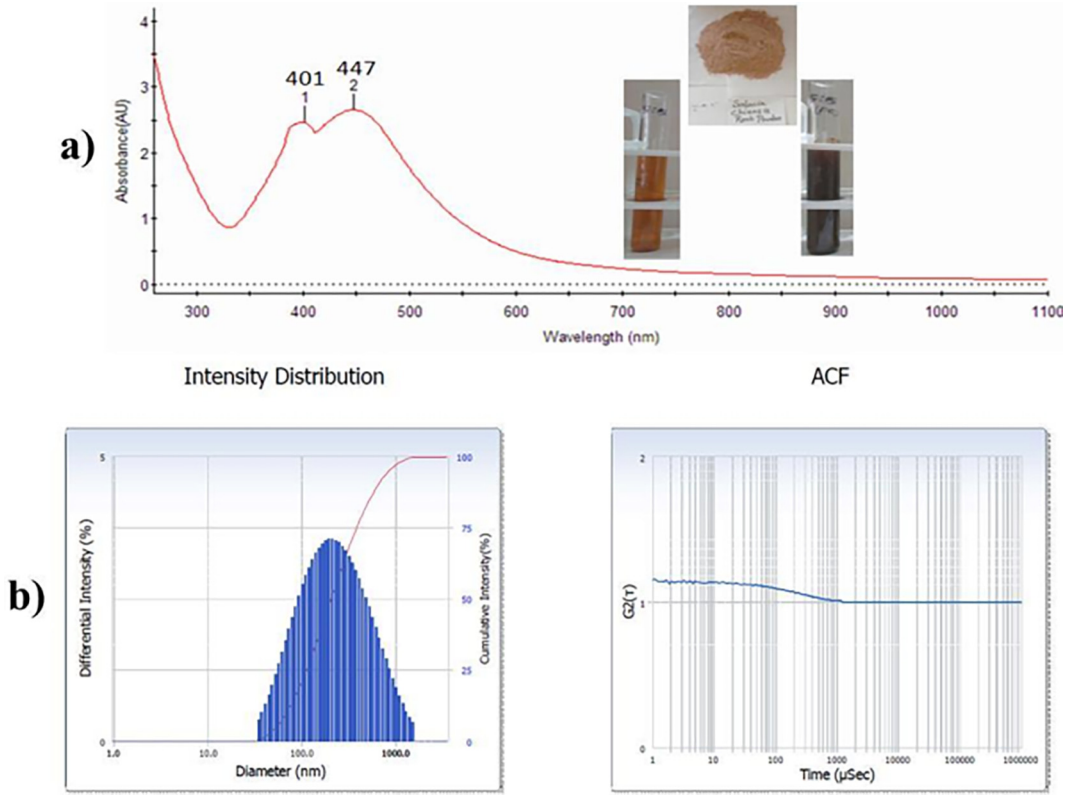


**Fig. 1.** a) UV–Vis spectra of *Sc*-AgNPs; b) Nanoparticle size measurements and PDI analysis.

nols, alkaloids, tannins, and steroids correspond to the major absorption bands and significant observation of synthesized *Sc*-AgNPs. These results are consistent, with signify of the phytocompounds that act as capping agents for synthesize *Sc*-AgNPs.

### 3.1.4. XRD diffraction pattern

(Fig. 2B) shows the XRD diffraction pattern plane of the synthesized *Sc*-AgNPs. Various peaks at 2θ values of at 28.78, 32.18, 38.04, 54.63, and 77.08°, which was conforming to the (111), (200), (120), (220), and (311) planes. Accordingly, the crystalline structure was reflected on the synthesized *Sc*-AgNPs. XRD pattern was similar to biosynthesized AgNPs from leaves of *Cucumis prophetarum* L. The face-centered cubic patterns of *Cucumis prophetarum* L. AgNPs were reflected by these predominant spectrum peaks. The high peaks of the planes (111, 200, and 311) were also recorded in *Cucumis prophetarum* L. AgNPs that were biosynthesized (Jebril et al., 2020).

### 3.1.5. SEM image

The particle shape and size of *Sc*-AgNPs were seen via SEM analysis. (Fig. 2 C) shows that spherical shape average size 8 nm with inter-particle dispersion. The results revealed unique spherical and poly-dispersed particles with a modest size and little aggregation. The results exhibited a range of values comparable with published data (Behravan et al., 2019; Mohammed et al., 2018; Balan et al., 2021; Sukweenadhi et al., 2021). Furthermore, scanning electron microscopy (SEM), which uses electron beams as imaging probes, is being used to evaluate nanoparticles surface appearance, size, aggregation, and dispersion. It offers high-resolution pictures at the nanoscale scale and information on the function of biomatrix of *Sc*-AgNPs.

### 3.2. Antimicrobial activity

The antimicrobial potential of biosynthesized *Sc*-AgNPs was tested against a variety of selected four bacterial and two fungal pathogenic strains. The measurement of zone of growth inhibition was compared to that achieved with conventional antibiotics. The four bacterial pathogens Gram positive (*Staphylococcus aureus*, *Proteus vulgaris, Streptococcus pyogenes*), Gram negative (*Escherichia coli*) and two pathogenic fungi (*Aspergillus niger* and *Candida albicans*) (Table 1), (Fig. 3A and B). The inhibitory zone ranged from 9 to 19.5 mm. The largest zone of inhibition was obtained against *Staphylococcus aureus* and *Proteus vulgaris* with *Sc*-AgNPs concentrations of 500 µg $mL^{-1}$ (19.5 mm). However, the *Sc*-AgNPs was low inhibition against *Escherichia coli.* In terms of cell wall composition, gram-positive cells have a higher inhibitory effect zone than gram negative cells (Yarrappagaari et al., 2020). Gram-positive cell wall comprises bushy layers of peptidoglycan and linear polysaccharide chains, whereas Gram-negative bacterial cell wall is more complex structurally (Bharathi et al., 2018). Conversely, maximum inhibition zone against Candida albicans (13.5 mm). The results were directly compared with the previously reported findings on antimicrobial activity of *Capparis zeylanica* L. leaf extract synthesized *Sc*-AgNPs were tested against Gram negative (*Shigella dysenteriae*, Salmonella paratyphi) and Gram positive *(Staphylococcus epidermidis, Enterococcus faecalis),* bacteria and fungi (Aspergillus niger, Candida albicans). The highest diameter zone of inhibitory activity was observed in 30 mm, 26 mm, 23 mm and 20 mm against *Staphylococcus epidermidis, Enterococcus faecalis,* Salmonella Paratyphi, *Shigella dysenteriae* respectively and highest zone of inhibition was observed in fungi Candida albicans 25 mm and Aspergillus niger (23 mm) (Nilavukkarasi et al., 2020).

The antimicrobial activities mechanism of synthesized *Sc*-AgNPs may deals with the cell membrane, causing disruption

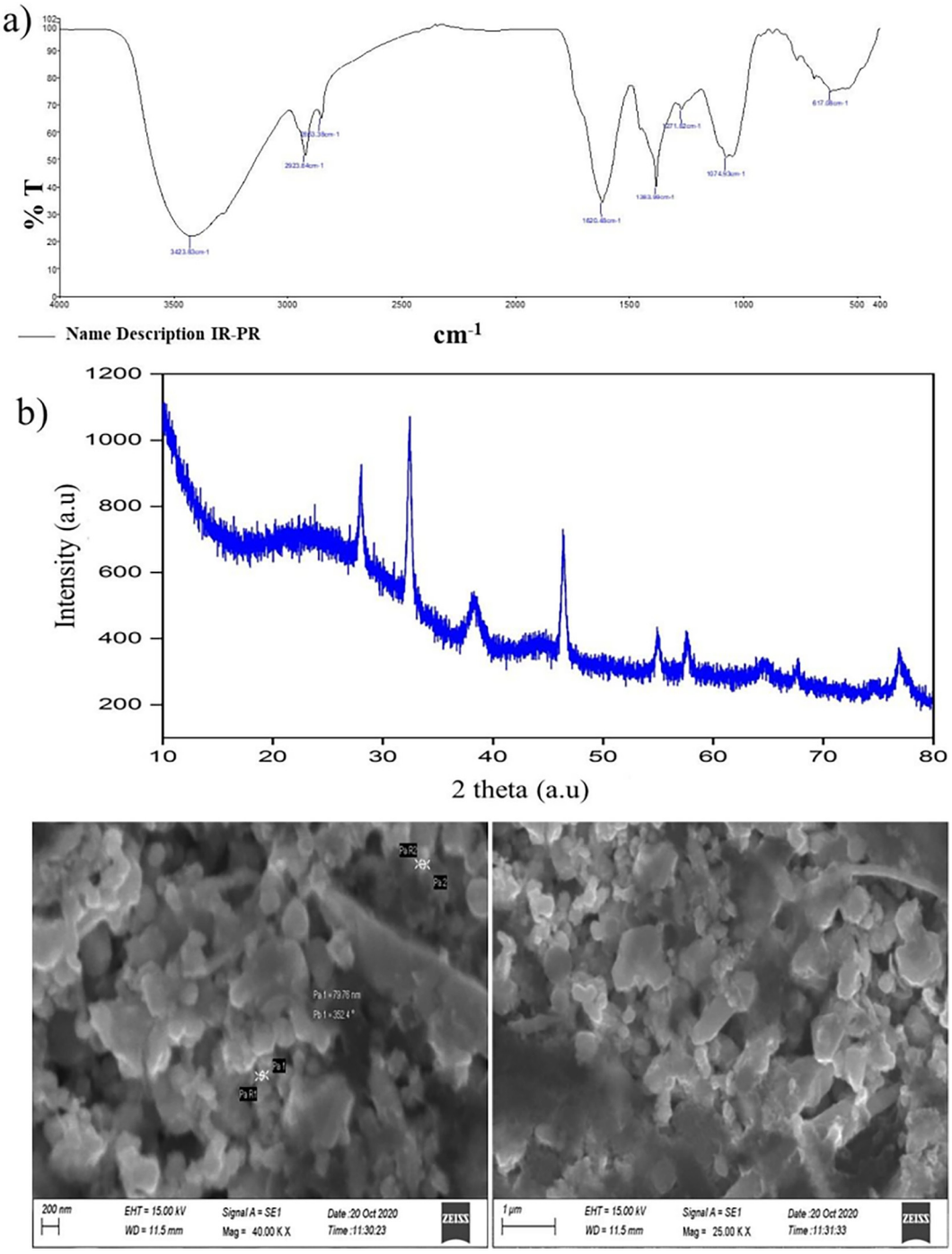


**Fig. 2.** a) FTIR spectra of the *Sc*-AgNPs; b) XRD pattern of the synthesized *Sc*-AgNPs; c) SEM image of *Sc*-AgNPs in scale bar of 200 nm.

**Table 1**
Antibacterial activity of various concentrations of *Sc*-AgNPs (inhibition of bacterial growth).

| S.No | Name of the test organism | Zone of inhibition (mm) SD ± Mean | | | | |
|---|---|---|---|---|---|---|
| | | 500 µg mL$^{-1}$ | 250 µg mL$^{-1}$ | 100 µg mL$^{-1}$ | 50 µg mL$^{-1}$ | PC |
| 1. | *Staphylococcus aureus* | 19.5 ± 0.5 | 18.5 ± 0.5 | 17.5 ± 0.5 | 16.5 ± 0.5 | 21 ± 1.0 |
| 2. | *Escherichia coli* | 14.5 ± 0.5 | 12.5 ± 0.5 | 11.5 ± 0.5 | 11.2 ± 0.2 | 19 ± 1.0 |
| 3. | *Proteus vulgaris* | 19.5 ± 0.5 | 16.5 ± 0.5 | 16.8 ± 0.3 | 14.5 ± 0.5 | 18 ± 1.0 |
| 4. | *Streptococcus pyogenes* | 15.5 ± 0.5 | 14.5 ± 0.5 | 10 ± 0.2 | 9.5 ± 0.5 | 19 ± 1.0 |

Mentioned values are mean and standard error of triplicates (±SE).

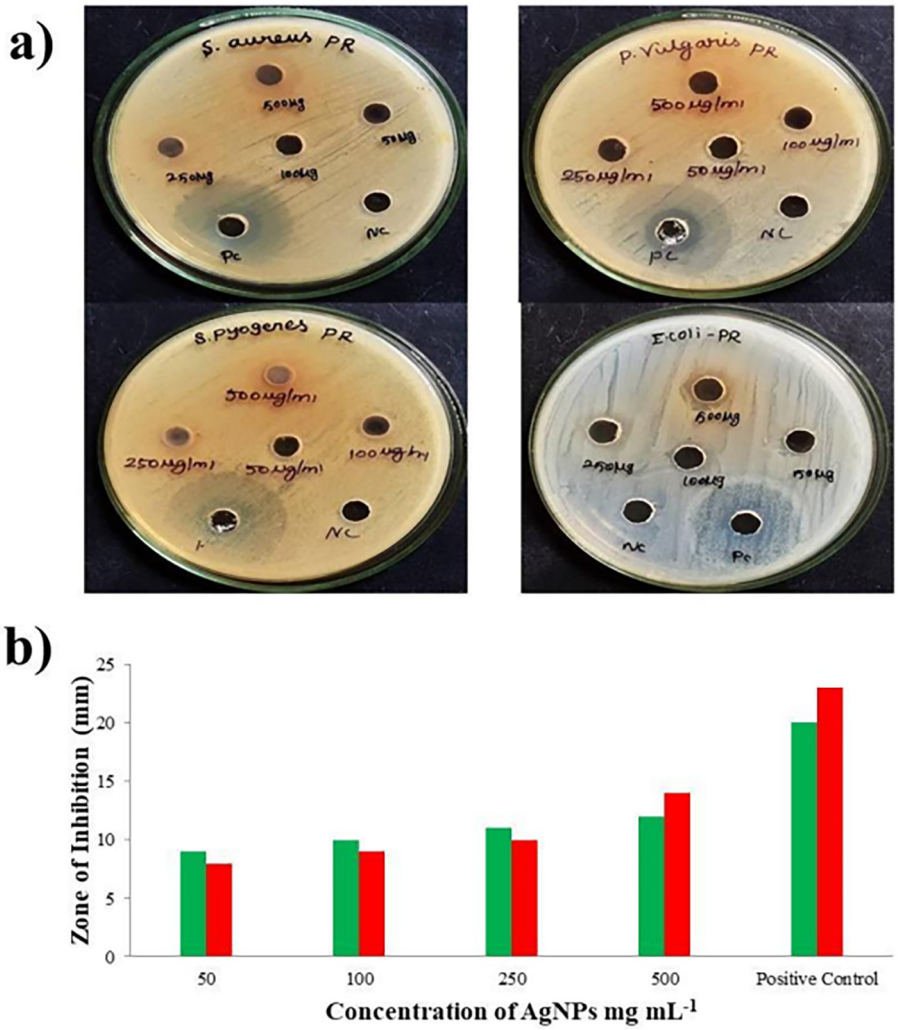


**Fig. 3.** A. a. Antibacterial activity of *Sc*-AgNPs (inhibition of bacterial growth) against *Staphylococcus aureus*, *Proteus vulgaris, Streptococcus pyogenes* and *Escherichia coli*; b. Antifungal activity of *Sc*-AgNPs (inhibition of mycelial growth) against *Aspergillus niger* (green bar) and *Candida albicans* (red bar).*mg mL*$^{-1}$.

and ultimately killing the bacterium (Hemlata et al., 2020), described the biosynthesized *Sc*-AgNPs first attachment to the cell membrane. Secondly, the cleavage and discharge of internal components (Proteins, DNA, and macromolecules), Finally, after entering the bacterial (Gram-positive and negative) cell wall, AgNPs release silver ions, which causing slow DNA damage and disrupting protein synthesis and the resulting failure of membrane permeability (Kubendiran et al., 2021). The antibacterial activity might be caused by a contact between small bacterial cells and *Sc*-AgNPs, which causes a metabolic inequity in microbes following *Sc*-AgNPs absorption, resulting the reactive oxygen species formation occurs, which kills bacteria. The quantity and morphological properties of *Sc*-AgNPs determine the antibacterial mechanism on microbes. When compared to larger particles; smaller nanoparticles have a higher proportion of interactions. Despite being more prone to dispersion than bigger particles, the smallest particles had the most against microbial pathogens. The size of nanoparticles influences their antibacterial effectiveness (Yin et al., 2020).

Antifungal elements are largely directed against fungus cellular components via mechanisms described (Scorzoni et al., 2017). First, the agents (nanoparticles) enter the fungus through cytosine permease in cell membrane. Second, inhibit the function of thymidylate synthetase in DNA replication, and interact with DNA, causing DNA damage, at the beginning of the fungicidal interaction of nano components.

### 3.3. Antioxidant activity using DPPH and ABTS assay

DPPH and ABTS tests were used to evaluate the antioxidant activity of the synthesized *Sc*-AgNPs *in vitro*. The analysis revealed that the DPPH and ABTS radical scavenging effect of the synthesized *Sc*-AgNPs was increased significantly in a dose-dependent mode of action, and ascorbic acid (Vitamin C) was served as a positive control.

### 3.4. Antioxidant activity using DPPH

Antioxidants can protect the cells against extremely reactive and unpredictable radicals. In this work, the synthesized *Sc*-AgNPs had the greatest free radical scavenging activity. The $IC_{50}$ value of -*Sc*-AgNPs against the DPPH radicals was found to be 117.3 μg mL$^{-1}$ and it was quite comparable with the ascorbic acid value (110.3 μg mL$^{-1}$) (Fig. 4A). The synthesized *Sc*-AgNPs had the greatest scavenging activity. The percentage of inhibition was estimated to be around 117.3 μg mL$^{-1}$. It was quite comparable to $IC_{50}$ value of vitamin C (110.3 g mL$^{-1}$). The varying concentration of the *Sc*-AgNPs (10, 20, 30, 40, 50, 100, 200, 300, 400 and 500 μg mL$^{-1}$) significantly (dose response inhibition) scavenged DPPH by 32.66, 34.10, 37.98, 40.52, 43.45, 45.14, 47.83, 51.83, 53.94, 58.79 and 95.39 % respectively. Because a compound percentage inhibition is related to its capacity to transport electrons, it may predict its

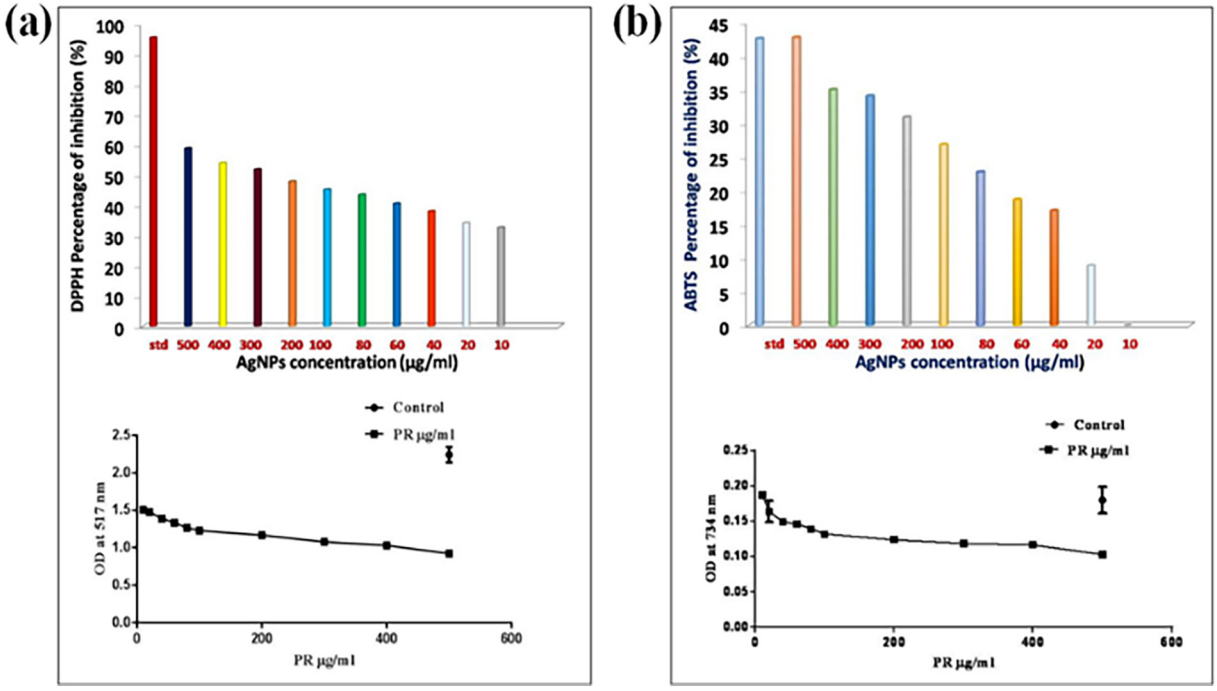


**Fig. 4.** a) DPPH activity on *Sc*-AgNPs Percentage of inhibition and Optical density Value at 517 nm; b) ABTS activity on *Sc*-AgNPs Percentage of inhibition and Optical density value at 734 nm.

prospective antioxidant activity (Vanlalveni et al., 2021). The phytochemicals in these synthesized silver nanoparticles may have efficiently provided the hydrogen molecule for this reaction due to a dose-dependent colour shift from clean violet to bright or yellowish dark brown matching the component 2,2- Diphenyl-1-picrylhydrazine. The synthesized *Sc*-AgNPs exhibited good antioxidant activity (58.79 %) in the DPPH scavenging assay at an $IC_{50}$ value of 117.3 g $mL^{-1}$, which was substantially compared with the standard (95.39 %). Furthermore, at $p < 0.03$ to $p < 0.05$, they were statistically significant.

### 3.5. ABTS assay

The antioxidant efficacy of *Sc*-AgNPs was evaluated using the ABTS radical cation scavenging assay. The oxidation of ABTS by potassium persulfate produces ABTS, a blue chromophore. The preformed cation radical is decreased in the presence of the plant extract. It makes use of a specific absorbance at 734 nm, a wavelength that is not visible, and has a quick reaction time. As the quantity of *Sc*-AgNPs rose, the ABTS cation radical scavenging activity increased. At concentrations ranging from 20 to

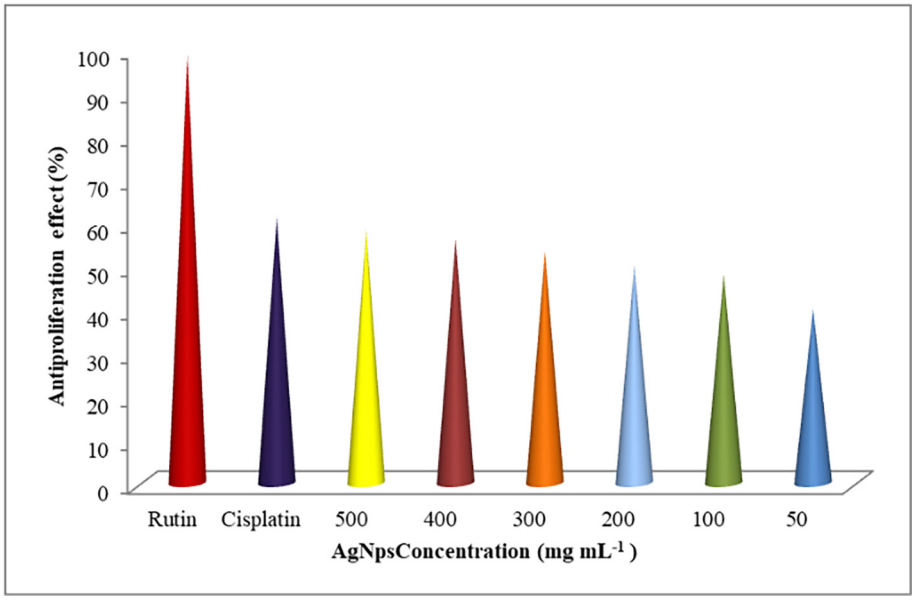


**Fig. 5.** Antiproliferation activity of *Sc*-AgNPs on HEK 293 kidney cell line.

500 μg $mL^{-1}$, ABTS cation radical scavenging activity ranged from 8.88 to 42.77 %. The $IC_{50}$ value was found as 59.61 g $mL^{-1}$ (Fig. 4B). This was quite similar to the $IC_{50}$ value of vitamin C (50.1 g $mL^{-1}$). The varying concentration of the *Sc*-AgNPs (10, 20, 30, 40, 50, 100, 200, 300, 400 and 500 μg $mL^{-1}$) significantly ABTS by 8.88, 17.03, 18.70, 22.77, 26.85, 30.92, 34.07, 35.00, 42.77 and 52.59 % respectively. The ability of the nanoparticles to absorb neutral and cationic radicals was tested, demonstrating that the *Sc*-AgNPs can absorb stable neutral radicals generated from ABTS. The numerous functional groups from the plant root extract responsible for the reduction and capping of the *Sc*-AgNPs may be linked to the observed free radical scavenging capacity of *Sc*-AgNPs when compared to ascorbic acid. This implies that this plant root extract *Sc*-AgNPs might be used as a substitute antioxidant in treating free-radical connected illnesses.

### 3.6. Antiproliferation activity

(Fig. 5) reveals that, HEK293 percentage of antiproliferation activity of the bio synthesized Ag NPs increased with various concentrations as 34.5 –97.4 %, it had a statistical significance of $p < 0.03$. The results showed that a concentration of 500 g $mL^{-1}$ of the synthesized *Sc*-AgNPs may protect up to 90.3 % against of Human Embryonic Kidney cell lines. Surprisingly, it had a high correlation with the positive control rutin (97.4 %). In general, frequent consumption of different formulations of drug candidates, such as cisplatin, renal failure with high serum creatinine and urea levels might occur, and increase the formation of ROS, resulting in the initiation of the interleukin 1L-1 synthesis (mediator for inflammation), (TNF-α), and signalling pathways, as well as the regular pathways complications (Thirumalaisamy et al., 2018). As a result, oxidative stress is a significant contributor to cell death. In this work, the positive control greatly protected the cells from nephrotoxicity (up to 97.4 %). Similarly, Liu et al. observed that high concentration of silver nanoparticles (AgNPs) indicates the apoptosis against HEK293 (Liu et al., 2021).

## 4. Conclusion

This analysis leads to some useful conclusions, most important of which, the potent therapeutic phytochemicals concerned in plant-based nanoparticle fabrications are biocompatible for various biological purposes. Green synthesis of *Sc*-AgNPs employing *Salacia chinensis* L. ethanolic root extract as a reducing and capping agent able to reduce silver ions into *Sc*-AgNPs without the use of harsh conditions. In a dose-dependent manner, the produced silver nanoparticles were examined for antibacterial activity against pathogenic bacteria and fungus, as well as antiproliferative effects on human embryonic kidney cell lines. In an overall conclusion, this study offers another dimension to the medicinal hub plant *Salacia chinensis* L. Its capacity to successfully synthesize *Sc*-AgNPs may improve antioxidant defense mechanisms and could also be utilized in the pharmaceutical industry.

## Declaration of Competing Interest

The authors declare that they have no known competing financial interests or personal relationships that could have appeared to influence the work reported in this paper.

## Acknowledgement

The authors are grateful to the Researchers supporting project number (RSP-2021/360), King Saud University, Riyadh, Saudi Arabia.

## Appendix A. Supplementary data

Supplementary data to this article can be found online at https://doi.org/10.1016/j.jksus.2022.102284.

## References

Al-Otibi, F., Perveen, K., Al-Saif, N.A., Alharbi, R.I., Bokhari, N.A., Albasher, G., Al-Otaibi, R.M., Al-Mosa, M.A., 2021. Biosynthesis of silver nanoparticles using *Malva parviflora* and their antifungal activity. Saudi J. Biol. Sci. 28, 2229–2235. https://doi.org/10.1016/j.sjbs.2021.01.012.

Balan, L., Chandrasekaran, S., Gajendiran, M., Nanjian, R., 2021. Synthesis of silver nanoparticles from *Pedalium murex* L. and its antiproliferative activity against breast cancer (MCF-7) cells. J. Mol. Struct. 1242 (1306). https://doi.org/10.1016/j.molstruc.2021.130695.

Behravan, M., Panahi, A.H., Naghizadeh, A., Ziaee, M., Mahdavi, R., Mirzapour, A., 2019. Facile green synthesis of silver nanoparticles using *Berberis vulgaris* leaf and root aqueous extract and its antibacterial activity. Int. J. Biol. Macromol. 124, 148–154. https://doi.org/10.1016/j.ijbiomac.2018.11.101.

Bharathi, D., Diviya Josebin, M., Vasantharaj, S., Bhuvaneshwari, V., 2018. Biosynthesis of silver nanoparticles using stem bark extracts of *Diospyros montana* and their antioxidant and antibacterial activities. J. Nanostructure Chem. 8, 83–92. https://doi.org/10.1007/s40097-018-0256-7.

Cassir, N., Rolain, J.M., Brouqui, P., 2014. A new strategy to fight antimicrobial resistance: the revival of old antibiotics. Frontiers Microbiol. 5, 1–16. https://doi.org/10.3389/fmicb.2014.00551.

Chinnappan, S., Kandasamy, S., Arumugam, S., Seralathan, K.K., Thangaswamy, S., Muthusamy, G., 2018. Biomimetic synthesis of silver nanoparticles using flower extract of *Bauhinia purpurea* and its antibacterial activity against clinical pathogens. Environ. Sci. Pollut. Res. 25, 963–969. https://doi.org/10.1007/s11356-017-0841-1.

Del-Toro-Sánchez, C.L., Rodríguez-Félix, F., Cinco-Moroyoqui, F.J., Juárez, J., Ruiz-Cruz, S., Wong-Corral, F.J., Borboa-Flores, J., Castro-Enríquez, D.D., Barreras-Urbina, C.G., Tapia-Hernández, J.A., 2021. Recovery of phytochemical from three safflower (*Carthamus tinctorius* L.) by-products: Antioxidant properties, protective effect of human erythrocytes and profile by uplc-dad-ms. J. Food Process. Preserv. 45 (9). https://doi.org/10.1111/jfpp.15765.

Egbuna, C., Awuchi, C.G., Kushwaha, G., Rudrapal, M., Patrick-Iwuanyanwu, K.C., Singh, O., Odoh, U.E., Khan, J., Jeevanandam, J., Kumarasamy, S., Chukwube, V.O., Narayanan, M., Palai, S., Găman, M.-A., Uche, C.Z., Ogaji, D.S., Ezeofor, N.J., Mtewa, A.G., Patrick-Iwuanyanwu, C.C., Kesh, S.S., Shivamallu, C., Saravanan, K., Tijjani, H., Akram, M., Ifemeje, J.C., Olisah, M.C., Chikwendu, C.J., 2021. Bioactive compounds effective against type 2 diabetes mellitus: a systematic review. Cur. Topics Med. Chem. 21 (12), 1067–1095.

Gacem, M.A., Telli, A., Gacem, H., Ould-El-Hadj-Khelil, A., 2019. Phytochemical screening, antifungal and antioxidant activities of three medicinal plants from *Algerian steppe* and Sahara (preliminary screening studies). SN Applied Sci. 1, 1–13. https://doi.org/10.1007/s42452-019-1797-1.

Gonfa, Y.H., Beshah, F., Tadesse, M.G., Bachheti, A., Bachheti, R.K., 2021. Phytochemical investigation and potential pharmacologically active compounds of *Rumex nepalensis*: an appraisal. Beni-Suef Univ. J. Basic Appl. Sci. 10, 1–15. https://doi.org/10.1186/s43088-021-00110-1.

Gour, A., Jain, N.K., 2019. Advances in green synthesis of nanoparticles. Artif Cells Nanomed. Biotechnol. 47, 844–851. https://doi.org/10.1080/21691401.2019.1577878.

Hemlata, Meena, P.R., Singh, A.P., Tejavath, K.K., 2020. Biosynthesis of silver nanoparticles using *Cucumis prophetarum* aqueous leaf extract and their antibacterial and antiproliferative activity against cancer cell lines. ACS Omega 5 (10), 5520–5528.

Jain, S., Mehata, M.S., 2017. Medicinal plant leaf extract and pure flavonoid mediated green synthesis of silver nanoparticles and their enhanced antibacterial property. Sci. Rep. 7, 1–13. https://doi.org/10.1038/s41598-017-15724-8.

Jebril, S., Jenana, R.K.B., Dridi, C., 2020. Green synthesis of silver nanoparticles using *Melia azedarach* leaf extract and their antifungal activities: *In vitro* and *in vivo*. Mater. Chem. Phys. 248,. https://doi.org/10.1016/j.matchemphys.2020.122898 122898.

Kartini, K., Alviani, A., Anjarwati, D., Fanany, A.F., Sukweenadhi, J., Avanti, C., 2020. Process Optimization for Green Synthesis of Silver Nanoparticles Using Indonesian Medicinal Plant Extracts. Processes. 8 (8), 998. https://doi.org/10.3390/pr8080998.

Kebede, T., Gadisa, E., Tufa, A., Karunasagar, I., 2021. Antimicrobial activities evaluation and phytochemical screening of some selected medicinal plants: A possible alternative in the treatment of multidrug-resistant microbes. PLoS One. 16 (3). https://doi.org/10.1371/journal.pone.0249253.

Keerawelle, B.I., Chamara, A.M., Thiripuranathar, G., 2019. Green synthesis of silver nanoparticles via medicinal plant extracts and their antibacterial activities. World J. Pharm. Res. 8 (7), 100–111. https://doi.org/10.20959/wjpr20197-15074.

Khan, F., Iqbal, S., Khalid, N., Hussain, I., Hussain, Z., Szmigielski, R., Janjua, H.A., 2020. Screening and stability testing of commercially applicable *Heliotropium crispum* silver nanoparticle formulation with control over aging and biostability. Appl. Nanosci. 10, 1941–1956. https://doi.org/10.1007/s13204-020-01333-x.

Kubendiran, L., Theerthagiri, S., Al-Dhabi, N.A., Palaninaicker, S., Subramanian, S.M., Srinivasan, V., Karuppiah, P., 2021. *In vitro* preparation of biosurfactant based herbal-nano topical ointment from *Tridax procumbens* infused oil using gelatin stabilized silver nanoparticle and its efficacy on fibroblastic cell lines. Appl. Nanosci. https://doi.org/10.1007/s13204-021-01896-3.

Lee, K.J., Park, S.H., Govarthanan, M., Hwang, P.H., Seo, Y.S., Cho, M., Lee, W.H., Lee, J. Y., Kamala-Kannan, S., Oh, B.T., 2013. Synthesis of silver nanoparticles using cow milk and their antifungal activity against phytopathogens. Mater. Lett. 105, 128–131. https://doi.org/10.1016/j.matlet.2013.04.076.

Liu, X., Shan, K., Shao, X., Shi, X., He, Y., Liu, Z., Jacob, J.A., Deng, L., 2021. Nanotoxic effects of silver nanoparticles on normal HEK-293 cells in comparison to cancerous HeLa cell line. Int. J. Nanomedicine. 16, 753–761.

Mohammed, A.E., Bin Baz, F.F., Albrahim, J.S., 2018. *Calligonum comosum* and *Fusarium sp*. extracts as bio-mediator in silver nanoparticles formation: characterization, antioxidant and antibacterial capability. Biotech. 8, 1–14. https://doi.org/10.1007/s13205-017-1046-5.

Narayanan, M., Gopi, A., Natarajan, D., Kandasamy, S., Saravanan, M., El Askary, A., Elfasakhany, A., Pugazhendhi, A., 2021. Hepato and nephroprotective activity of methanol extract of *Hygrophila spinosa* and its antibacterial potential against multidrug resistant *Pandoraea sputorum*. Environ. Res. 201,. https://doi.org/10.1016/j.envres.2021.111594 111594.

Nguyen, D.H., Lee, J.S., Park, K.D., Ching, Y.C., Nguyen, X.T., Phan, V.H., Hoang Thi, T. T., 2020. Green silver nanoparticles formed by *Phyllanthus urinaria*, *Pouzolzia zeylanica*, and *Scoparia dulcis* leaf extracts and the antifungal activity. Nanomaterials. 10, 1–13. https://doi.org/10.3390/nano10030542.

Nilavukkarasi, M., Vijayakumar, S., Kumar, S.P., 2020. Biological synthesis and characterization of silver nanoparticles with *Capparis zeylanica* L. leaf extract for potent antimicrobial and anti proliferation efficiency. Mater. Sci. Energy Technol. 3, 371–376. https://doi.org/10.1016/j.mset.2020.02.008.

Reda, M., Ashames, A., Edis, Z., Bloukh, S., Bhandare, R., Abu Sara, H., 2019. Green synthesis of potent antimicrobial silver nanoparticles using different plant extracts and their mixtures. Processes. 7, 1–14. https://doi.org/10.3390/pr7080510.

Rodríguez-Félix, F., López-Cota, A.G., Moreno-Vásquez, M.J., Graciano-Verdugo, A.Z., Quintero-Reyes, I.E., Del-Toro-Sánchez, C.L., Tapia-Hernández, J.A., 2021. Sustainable-green synthesis of silver nanoparticles using safflower (*Carthamus tinctorius* L.) waste extract and its antibacterial activity. Heliyon 7 (4), e06923.

Rodríguez-Félix, F., Graciano-Verdugo, A.Z., Moreno-Vásquez, M.J., Lagarda-Díaz, I., Barreras-Urbina, C.G., Armenta-Villegas, L., Olguín-Moreno, A., Tapia-Hernández, J.A., Yi, D.K., 2022. Trends in sustainable green synthesis of silver nanoparticles using agri-food waste extracts and their applications in health. J. Nanomater. 2022, 1–37.

Samuggam, S., Chinni, S.V., Mutusamy, P., Gopinath, S., Anbu, P., Venugopal, V., Reddy, L.V., Enugutti, B., 2021. Green Synthesis and Characterization of Silver Nanoparticles Using *Spondias mombin* Extract and Their Antimicrobial Activity against Biofilm-Producing Bacteria. *Molecules* (Basel, Switzerland) 26 (9), 2681. https://doi.org/10.3390/molecules26092681.

Scorzoni, L., de Paula e Silva, A.C.A., Marcos, C.M., Assato, P.A., de Melo, W.C.M.A., de Oliveira, H.C., Costa-Orlandi, C.B., Mendes-Giannini, M.J.S., Fusco-Almeida, A.M., 2017. Antifungal therapy: new advances in the understanding and treatment of mycosis. Front. Microbiol. 08. https://doi.org/10.3389/fmicb.2017.00036.

Sudhakar, C., Selvam, K., Govarthanan, M., Senthilkumar, B., Sengottaiyan, A., Stalin, M., Selvankumar, T., 2015. *Acorus calamus* rhizome extract mediated biosynthesis of silver nanoparticles and their bactericidal activity against human pathogens. J. Genet. Eng. Biotechnol. 13, 93–99. https://doi.org/10.1016/j.jgeb.2015.10.003.

Sukweenadhi, J., Setiawan, K.I., Avanti, C., Kartini, K., Rupa, E.J., Yang, D.C., 2021. Scale-up of green synthesis and characterization of silver nanoparticles using ethanol extract of *Plantago major* L. leaf and its antibacterial potential. S. Afr. J. Chem. Eng. 38, 1–8. https://doi.org/10.1016/j.sajce.2021.06.008.

Tapia-Hernández, J.A., Rodríguez-Felix, F., Juárez-Onofre, J.E., Ruiz-Cruz, S., Robles-García, M.A., Borboa-Flores, J., Wong-Corral, F.J., Cinco-Moroyoqui, F.J., Castro-Enríquez, D.D., Del-Toro-Sánchez, C.L., 2018. Zein-polysaccharide nanoparticles as matrices for antioxidant compounds: A strategy for prevention of chronic degenerative diseases. Food Res. Int. 111, 451–471. https://doi.org/10.1016/j.foodres.2018.05.036.

Tapia-Hernández, J.A., Del-Toro-Sánchez, C.L., Cinco-Moroyoqui, F.J., Ruiz-Cruz, S., Juárez, J., Castro-Enríquez, D.D., Barreras-Urbina, C.G., López-Ahumada, G.A., Rodríguez-Félix, F., 2019b. b. Gallic acid-loaded zein nanoparticles by electrospraying process. J. Food Sci. 84 (4), 818–831. https://doi.org/10.1111/1750-3841.14486.

Tapia-Hernández, J.A., Del-Toro-Sánchez, C.L., Cinco-Moroyoqui, F.J., Juárez-Onofre, J.E., Ruiz-Cruz, S., Carvajal-Millan, E., López-Ahumada, G.A., Castro-Enriquez, D. D., Barreras-Urbina, C.G., Rodríguez-Felix, F., 2019a. Prolamins from Cereal By-products: Classification, Extraction, Characterization and its Applications in Micro- and Nanofabrication. Trends Food Sci. Technol. 90, 111–132. https://doi.org/10.1016/j.tifs.2019.06.005.

Thirumalaisamy, R., Ammashi, S., Muthusamy, G., 2018. Screening of anti-inflammatory phytocompounds from *Crateva adansonii* leaf extracts and its validation by *in silico* modeling. J. Genet. Eng. Biotechnol. 16, 711–719. https://doi.org/10.1016/j.jgeb.2018.03.004.

Vanlalveni, C., Lallianrawna, S., Biswas, A., Selvaraj, M., Changmai, B., Rokhum, S.L., 2021. Green synthesis of silver nanoparticles using plant extracts and their antimicrobial activities: a review of recent literature. RSC Adv. 11, 2804–2837. https://doi.org/10.1039/D0RA09941D.

Vijayakumar, N., Bhuvaneshwari, V.K., Ayyadurai, G.K., Jayaprakash, R., Gopinath, K., Nicoletti, M., Alarifi, S., Govindarajan, M., 2022. Green synthesis of zinc oxide nanoparticles using *Anoectochilus elatus*, and their biomedical applications. Saudi J. Biol. Sci. 29 (4), 2270–2279.

Yarrappagaari, S., Gutha, R., Narayanaswamy, L., Thopireddy, L., Benne, L., Mohiyuddin, S.S., Vijayakumar, V., Saddala, R.R., 2020. Eco-friendly synthesis of silver nanoparticles from the whole plant of *Cleome viscosa* and evaluation of their characterization, antibacterial, antioxidant and antidiabetic properties. Saudi J. Biol. Sci. 27, 3601–3614. https://doi.org/10.1016/j.sjbs.2020.07.034.

Yin, I.X., Zhang, J., Zhao, I.S., Mei, M.L., Li, Q., Chu, C.H., 2020. The antibacterial mechanism of silver nanoparticles and its application in dentistry. Int. J. Nanomedicine. 15, 2555–2562. https://dx.doi.org/10.2147%2FIJN.S246764.